Reconstruction of Incomplete Cell Paths through a 3D-2D Level Set Segmentation

Maia Hariri[a] and Justin W.L. Wan[a,b]

[a]Centre for Computational Mathematics in Industry and Commerce, University of Waterloo, 200 University Ave. West, Waterloo, ON, Canada;
[b]David R. Cheriton School of Computer Science, University of Waterloo, 200 University Ave. West, Waterloo, ON, Canada.

ABSTRACT

Segmentation of fluorescent cell images has been a popular technique for tracking live cells. One challenge of segmenting cells from fluorescence microscopy is that cells in fluorescent images frequently disappear. When the images are stacked together to form a 3D image volume, the disappearance of the cells leads to broken cell paths. In this paper, we present a segmentation method that can reconstruct incomplete cell paths. The key idea of this model is to perform 2D segmentation in a 3D framework. The 2D segmentation captures the cells that appear in the image slices while the 3D segmentation connects the broken cell paths. The formulation is similar to the Chan-Vese level set segmentation which detects edges by comparing the intensity value at each voxel with the mean intensity values inside and outside of the level set surface. Our model, however, performs the comparison on each 2D slice with the means calculated by the 2D projected contour. The resulting effect is to segment the cells on each image slice. Unlike segmentation on each image frame individually, these 2D contours together form the 3D level set function. By enforcing minimum mean curvature on the level set surface, our segmentation model is able to extend the cell contours right before (and after) the cell disappears (and reappears) into the gaps, eventually connecting the broken paths. We will present segmentation results of C2C12 cells in fluorescent images to illustrate the effectiveness of our model qualitatively and quantitatively by different numerical examples.

Keywords: Fluorescence microscopy, cell, 3D segmentation, level set method

1. INTRODUCTION

The study of cells is crucial in the development of science. Diseases like cancer are direct consequences of cell mutations such as rapid cell growth, abnormal cell division, and large quantities of cell death. For this reason, biologists consistently rely on live cell imaging via light microscopy for medical research and monitoring of diseases. The idea is to use visible light to detect and enlarge small objects such as cells inside a given frame. With this research tool, cell biologists can extract detailed images of the interrelated structures and dynamics of biological systems.

Fluorescent microscopy is one of the several types of imaging techniques used by these biologists to study cell movement, cell growth, cell metabolism, cell differentiation, and cell death.[1] Images from fluorescent microscopy are recorded in a time series, for example, taken every thirty minutes over a period of seven days. Typical experiments result in hundreds of images, each containing many cells that undergo movement, division, growth, and death, which render manual analysis extremely meticulous and time-consuming.[2]

In fluorescent microscopy, the cells are tagged with a protein that exhibits fluorescence when exposed to light of different wavelengths. The fluorophore is the component of the protein that causes the molecule to be fluorescent. The result is an image in which the objects of interest, usually the nuclei of the cells, are easily distinguishable from the background because they appear as bright convex shapes. However, the amount of energy emitted by the fluorophores depends on the environment they are in. Therefore it is sometimes possible for the protein to not emit a visible light when the cell undergoes chemical changes during its division cycle.

Further author information, send correspondence to Justin W.L. Wan. Email: jwlwan@uwaterloo.ca; phone 1 519 888 4567 ext 34468, fax: 1 519 885 1208

Medical Imaging 2012: Image Processing, edited by David R. Haynor, Sébastien Ourselin,
Proc. of SPIE Vol. 8314, 83141O · © 2011 SPIE · CCC code: 0277-786X/11/$18 · doi: 10.1117/12.911160

This property of fluorophores causes the cell to be missing from the frame of interest for a short period of time. Hence, given a sequence of fluorescent microscopy cell images obtained over a certain time interval, it is easy to locate the positions of the various objects in each frame. The problem lies in tracking the origin of a cell when it reappears into the frame after disappearing for a short period of time. Although this is a problem that is often mentioned in the literature, a solution that does not involve manual intervention has not yet been addressed.

It poses a challenge when tracking cells in fluorescent images, which has not been addressed much in the literature. When a cell disappears, it is not known when and where the cell will appear again. When a cell reappears, it is not easy to determine where it was. One confusion is whether this cell corresponds to a nearby cell from the previous frame, or it corresponds to a cell that disappeared a number of frames before. It is not apparent which disappearing cells correspond to which reappearing cells. Manually tracking these cells can be very time consuming. It is desirable that a robust cell tracker can handle these cases automatically.

Image segmentation[3–6] is a common tool used in the automated algorithm of cell tracking. A common challenge for programmers is to develop a segmentation method that is able to detect edges as accurately as the human eye, despite gaps and broken boundaries in the actual image. The standard tracking methods involve recording position and boundary information of the cells, at specified regular time intervals, using an appropriate segmentation technique. The identified boundaries in a given frame are then used as initial guesses for the position of the cells in the following frame.[7] In the case of a cell disappearing and reappearing, it is up to a specialist to identify the origin of the cell.

The segment-and-track method only uses information from the previous image frame. However, the entire sequence of recorded fluorescent images is often available for analysis. In this paper, we will exploit the temporal information of the cells in order to reconstruct the missing segments when a cell disappears from the frame. The set of images obtained from fluorescent microscopy are stacked in chronological order to create a three-dimensional image volume. The sequence of cells form"tubes" in the image volume; for example, the stacking of one cell is shown in Figure 1 (left). We define the case of a cell disappearing from the frame of interest, which can be seen in Figure 1 (right), as an incomplete cell path because there is a gap in the 3D image volume. Applying a three-dimensional segmentation to the volume will capture the cell tubes and hence the locations of the cells at different times. However, this approach alone does not resolve the issue of tracking a cell when it reappears into the frame after disappearing for some time. The standard 3D segmentation fails to connect the broken pieces together.

The goal of this paper is to develop a technique for reconstructing incomplete cell paths through a three-dimensional segmentation. The algorithm should automatically be able to bridge gaps that are easily detectable by the human eye in any image volume. The input parameters may vary from one experiment to another, however, within a single experiment, no adjustments to the parameters should be necessary. In this paper, we propose a 3D-2D segmentation model which performs 2D segmentation in a 3D framework. The 2D segmentation captures the cells that appear in the image frames while the 3D segmentation reconstructs the incomplete cell paths.

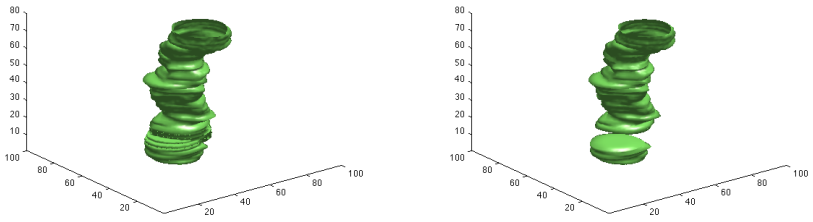

Figure 1. (Left) 3D segmentation of a complete cell path, (right) Disappearance of a cell from the frame of interest forms an incomplete cell path.

2. METHODOLOGY

Our approach is based on the active contour segmentation algorithm of Chan and Vese.[8] Level set methods[9] have the advantages of segmenting cells of different shapes, capturing naturally topological changes such as cell divisions, and easily extendable to three dimensions. Let Ω be an open bounded set in $\mathbb{R}^n$ with boundary $\partial\Omega$ that corresponds to the object that we wish to segment. A level set function ϕ is typically initialized as a signed distance function with the following properties:

$$\begin{aligned}
&\phi(\mathbf{x}(t),t) = 0 \quad \text{for } \mathbf{x} \in \partial\Omega \\
&\phi(\mathbf{x}(t),t) > 0 \quad \text{for } \mathbf{x} \in \Omega \\
&\phi(\mathbf{x}(t),t) < 0 \quad \text{for } \mathbf{x} \in \mathbb{R}^n \backslash (\Omega \cup \partial\Omega).
\end{aligned}$$

Thus, the boundary of the object, $\partial\Omega$, is given by the zero level set of ϕ.

2.1 Active contour segmentation

Assume that an image u can be separated into two regions of approximately piecewise-constant intensities, of distinct values u^{in}, which represents the object to be segmented, and u^{out}, which corresponds to the background of the image. In the three-dimensional implementation of the Chan-Vese model,[8] a level set function ϕ is used to divide u into two regions where $\phi > 0$ is the inside and $\phi < 0$ is the outside. Let c_{in} and c_{out} be the mean intensity values of the cell image region where $\phi > 0$ and $\phi < 0$, respectively. In three dimensions, the Chan-Vese model minimizes the energy functional:

$$\begin{aligned}
\min_{\phi} \quad & \mu \iiint_{\Omega} |\nabla H(\phi)| \, dxdydz \; + \; \nu \iiint_{\Omega} H(\phi) \, dxdydz \; + \; \lambda_1 \iiint_{\Omega} |u - c_{in}|^2 H(\phi) \, dxdydz \\
& + \lambda_2 \iiint_{\Omega} |u - c_{out}|^2 (1 - H(\phi)) \, dxdydz,
\end{aligned}$$

where $H(\cdot)$ is the Heaviside function, and μ, ν, λ_1 and λ_2 are parameters. The λ_1 and λ_2 terms are defined such that the energy is minimized when the level set surface is located right on the boundary of the object. The μ term is a regularization term to minimize the surface area and the ν term is to minimize the volume of the inside region. In the original Chan-Vese model, the volume term is ignored with ν chosen to be 0.

The corresponding Euler-Lagrange equation for ϕ is given by:

$$\frac{\partial \phi}{\partial t} = \delta(\phi) \left[\mu \nabla \cdot \left(\frac{\nabla \phi}{|\nabla \phi|} \right) - \nu - \lambda_1 (u - c_{in})^2 + \lambda_2 (u - c_{out})^2 \right], \tag{1}$$

where $\delta(\cdot)$ is the Dirac delta function and the initial contour is given by $\phi(x, y, z, 0) = \phi_0(x, y, z)$. At the steady state, the zero level set of ϕ gives the boundary of the object.

As illustrated in Figure 1 (right), the Chan-Vese level set segmentation is able to correctly capture the positions of the cell tubes when the cells are visible in the image frames. However, it would not be able to detect gaps in the cell tubes since the gaps are essentially the background.

2.2 3D-2D level set segmentation

The Chan-Vese model detects edges by comparing the intensity value at each voxel (x, y, z) with the mean intensity values inside and outside of the level set surface. However a point inside the gap of an incomplete cell path has the same intensity value as the background, as opposed to the intensity values within the cell tubes. Therefore, the level set surface will move away from the gap and simply capture the visible cells, as illustrated in Figure 2 (left). An important property of active contours without edges is that if $c_{in} = c_{out}$, that is the mean intensity values inside and outside the level function ϕ are equal, then the fitting terms is minimized for that particular ϕ. Furthermore, if $\nu = 0$, so that there is no volume constraint on the energy functional, then the level set surface will not evolve since the given ϕ is already an optimal solution. We use this particular property in our 3D-2D level segmentation method to avoid the undesirable motion of the level set surface moving away from the gap.

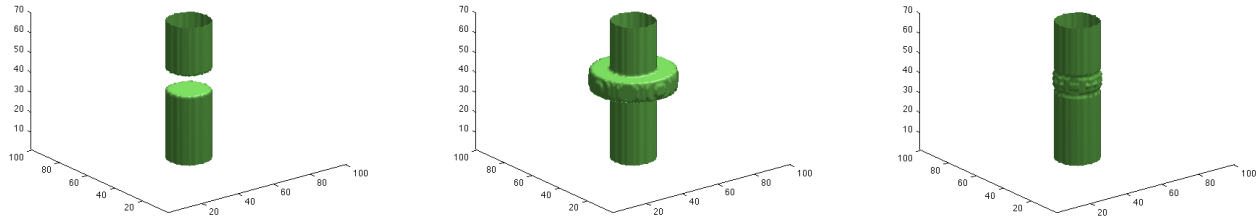

Figure 2. 3D segmentation of a cylinder with a gap of height 10 voxels given by the (left) Chan-Vese model, (middle) 3D-2D segmentation with $\mu = \nu = 0$, and (right) 3D-2D segmentation with $\mu, \nu \neq 0$.

In order to detect gaps in the z-direction, we propose that the comparison of the intensity values takes place at a two-dimensional slice instead of the three dimensional volume. More precisely, suppose we want to classify the voxel (x, y, z) as a point inside or outside the level set surface ϕ. We consider the image frame corresponding to the z position, say u^z, and project the 3D level set function ϕ onto frame z to obtain a 2D level set function:

$$\phi^z(x, y) = \phi(x, y, z).$$

This idea is illustrated in Figure 3. The image u is a cylinder that exhibits a gap between the slice $z = 50$ and $z = 60$. The zero level set surface of the initial level set function ϕ_0 is a sphere that encompasses the entire cylinder, including the gap. At any point on the 80th slice of u, denoted u^{80} (Figure 3 (left)), we consider the 2D level set function $\phi_0^{80}(x, y) = \phi_0(x, y, 80)$ for which the zero level set curve is shown in Figure 3 (middle).

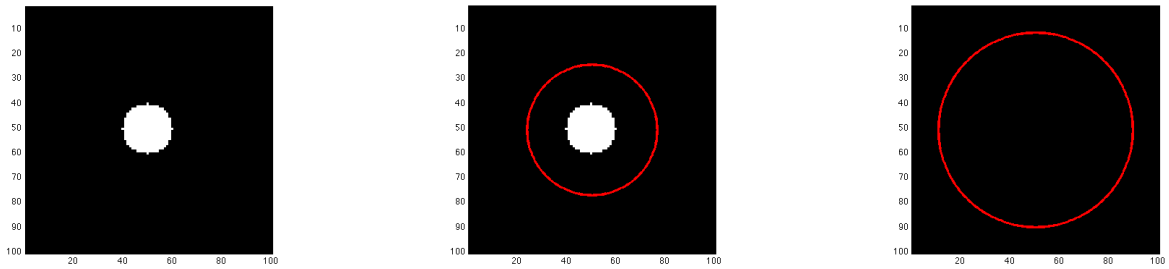

Figure 3. (Left) Frame 80 of the cylinder image u, (middle) projection of ϕ_0 onto frame 80, (right) projection of ϕ_0 onto frame 55 (inside the gap).

With this 2D projected level set function, we then define c_{in}^z and c_{out}^z to be the mean intensity values of u^z inside and outside ϕ^z, respectively. Instead of c_{in} and c_{out}, we will use c_{in}^z and c_{out}^z to determine whether the level set function ϕ should expand or shrink. Our proposed model equation for ϕ is given by

$$\frac{\partial \phi}{\partial t} = \delta(\phi) \left[\mu \nabla \cdot \left(\frac{\nabla \phi}{|\nabla \phi|} \right) - \nu - \lambda_1 (u - c_{in}^z)^2 + \lambda_2 (u - c_{out}^z)^2 \right].$$

This equation evolves the 3D level set function ϕ in such a way that it performs a 2D level set segmentation on each image frame. If a cell is present in an image frame z, as in Figure 3 (middle), the λ_1 and λ_2 terms will evolve ϕ and hence ϕ^z to capture the cell boundary. This is similar to the 2D Chan-Vese segmentation model. However, for an image frame within the gap of the volume such as in Figure 3 (right), c_{in}^z and c_{out}^z will be the same and the two λ terms will not cause ϕ to move. Thus, the zero level set surface will stay as the initial surface. As a result, it will not close the gap and split the cell tube into two as the standard Chan-Vese model does; see Figure 2 (center).

We note that the 3D-2D approach is not the same as segmenting each image frame individually. The latter would not be able to bridge the gap and would simply produce the same results as a three dimensional image segmentation. In our model, each 2D projected level set function ϕ^z locates the boundaries of the objects in its own image frame while maintaining information about the entire 3D level set function ϕ, In fact, this information is maintained by the regularization terms, μ and ν. For illustration purposes, consider a unique incomplete cell path with one gap. Suppose the cell is visible in frame z_1 but non-existent in the next frame $z_1 + 1$. Then the projected level set function ϕ^{z_1} is drastically different from ϕ^{z_1+1} because the first contour captures the cell in the 2D image whereas the second is given by the initial level set function. This large difference in contours induces a large mean curvature in the zero level set of ϕ. The regularization terms are meant to minimize this effect by evolving ϕ^{z_1+1} such that the contour will be close to the cell boundary given by ϕ^{z_1}. Hence, with an appropriate choice of μ and ν, the 3D-2D method will correctly capture the gap as in Figure 3 (right).

To summarize, the λ_1 and λ_2 terms drive the segmentation of the two-dimensional image towards the existing objects in the frame, capturing the visible parts of the cell tube. The regularization terms then extend the surface by minimizing the mean curvature into the region where the cell disappears, creating a segmentation of the missing cell. This method does not rely on physically identifying a gap region, it simply manipulates the level set surface to evolve in a desired manner when there is a gap within the embedding function. In other words, the level set curve is not attracted towards the gap, instead, it is designed to replicate contours from image frames prior to and following the gap.

3. NUMERICAL RESULTS

We apply the 3D-2D level set segmentation algorithm for cell images showing live C2C12 cells obtained from experiments performed at the Genomic Laboratory, McGill University. Due to limited space, we only show a few examples here to illustrate how the segmentation method works. All computation is performed on a Mac using MATLAB. The original image size is 512×512, but for illustration purpose, only the portion of a cell is shown whose size is around 100×100.

Figure 4 shows the results of the 3D-2D level set algorithm applied to an incomplete cell path containing one gap of height 8 voxels. A complete image dataset with the cell visible in each frame is taken as the ground truth. We then manually remove the cell from frames $z = 36$ to $z = 43$ to simulate the effect of a cell disappearing and reappearing from the frame of interest. For this experiment, we choose the 3D-2D parameters to be $\mu = 0.1$, $\nu = 1$, and $\lambda_1 = \lambda_2 = 1000$. The gap is visible in Figure 4 (left) which corresponds to an ordinary level set segmentation result. The 3D-2D level set method is able to reconstruct the incomplete cell path, as illustrated in Figure 4 (middle). In Figure 4 (right), we project the predicted segmentation surfaces onto frame 36 of the ground truth dataset; this corresponds to the actual cell. The segmentation contour agrees very well with the missing cell, capturing also the glow of the cell from the microscope.

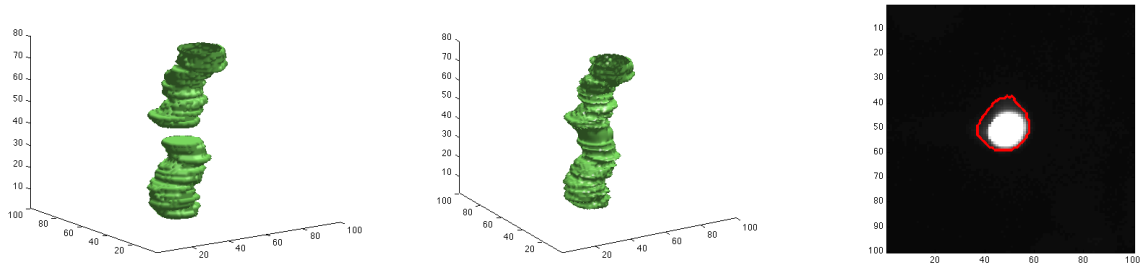

Figure 4. Segmentation results given by (left) the Chan-Vese model and (middle) the 3D-2D segmentation model. (Right) Projection of the predicted segmentation contour onto the ground truth.

Figure 5 shows that the 3D-2D segmentation method is capable of detecting multiple gaps of different sizes within one cell tube. Given the unicellular complete image dataset, we remove the cell from frames $z = 22$

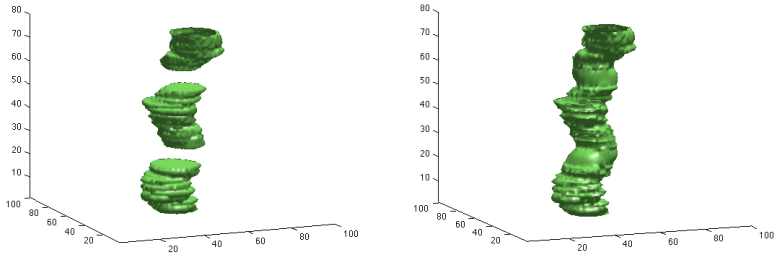

Figure 5. Segmentation results given by (left) the Chan-Vese model and (right) the 3D-2D segmentation model.

to $z = 29$ and from $z = 55$ to $z = 63$, as shown in Figure 5 (left). Once again, we observe an appropriate reconstruction of the incomplete cell path.

We demonstrate the effect of gap sizes on the segmentation results. An image dataset with all the cells visible is taken as the ground truth. We then manually remove a cell from 6, 11, and 16 frames, respectively. The 3D-2D segmentation is applied to reconstruct the incomplete cell path. The segmentation results for the image frames where a cell is missing are shown in Figure 6. The cell locations predicted by the 3D-2D segmentation (red contours) are ovelayed with the actual cell images that have been manually removed. In general, the segmentation contour agrees with the missing cell very well. The result is better for smaller gap sizes and tend to get worse when the gap size increases.

In another image sequence, we compute the accuracy of the 3D-2D segmentation for cells disappeared for 8 frames. Ten such cases are analyzed for a total of 80 image segmentation results. Accuracy is measured as $|A \cap B|/|A|$ where A denotes the segmentation result and B the ground truth. The results are shown in Figure 7. Reconstruction near the ends results in an accuracy of above 0.9 and decreases gradually in the middle since it is getting farther away from the known positions. However, on average, this method captures most of the missing cell with a mean accuracy of 87.5%.

Finally, we show the segmentation results for a 3D image volume containing multiple cells and two gaps. A complete image dataset with two cells in each frame is taken as the ground truth. We then manually remove a cell from frames $z = 16$ to $z = 22$ and a different one from frames $z = 60$ to $z = 66$, creating two gaps of size 7 voxels. For this experiment, we set $\mu = 0.02$ and $\nu = 2$. The gaps are visible in Figure 8 (upper left), which corresponds to the regular level set segmentation result. The 3D-2D segmentation method reconstructs the incomplete cell paths as shown in Figure 8 (upper right). In the 2D images, we show the segmentation results at slices $z = 17$ and $z = 61$. The green contour represents the segmentation of the cells that are visible in the image frame, whereas the red contour represents the predicted location of the missing cell. We observe that the 3D-2D segmentation method captures the cells quite accurately.

4. CONCLUSION

We have presented a segmentation model for reconstructing incomplete cell paths for tracking cells in fluorescent images when some of the cells disappear and reappear in the image sequence. By segmenting cells on 2D image frames in a 3D framework and enforcing minimum mean curvature on the level set surface, we have shown that our 3D-2D segmentation method is able to capture visible cells as well as cells that have disappeared. We have demonstrated the effectiveness of the model by a number of examples from different live cell images.

REFERENCES

[1] Rabut, G. and Ellenberg, J., "Automatic real-time three-dimensional cell tracking by fluorescence microscopy," *Journal of Microscopy* **216**, 131–137 (2004).

[2] Tse, S., Bradbury, L., Wan, J. W., Djambazian, H., Sladek, R., and Hudson, T., "A combined watershed and level set method for segmentation of brightfield cell images," in [*Proceedings of SPIE Medical Imaging*], (February 2009).

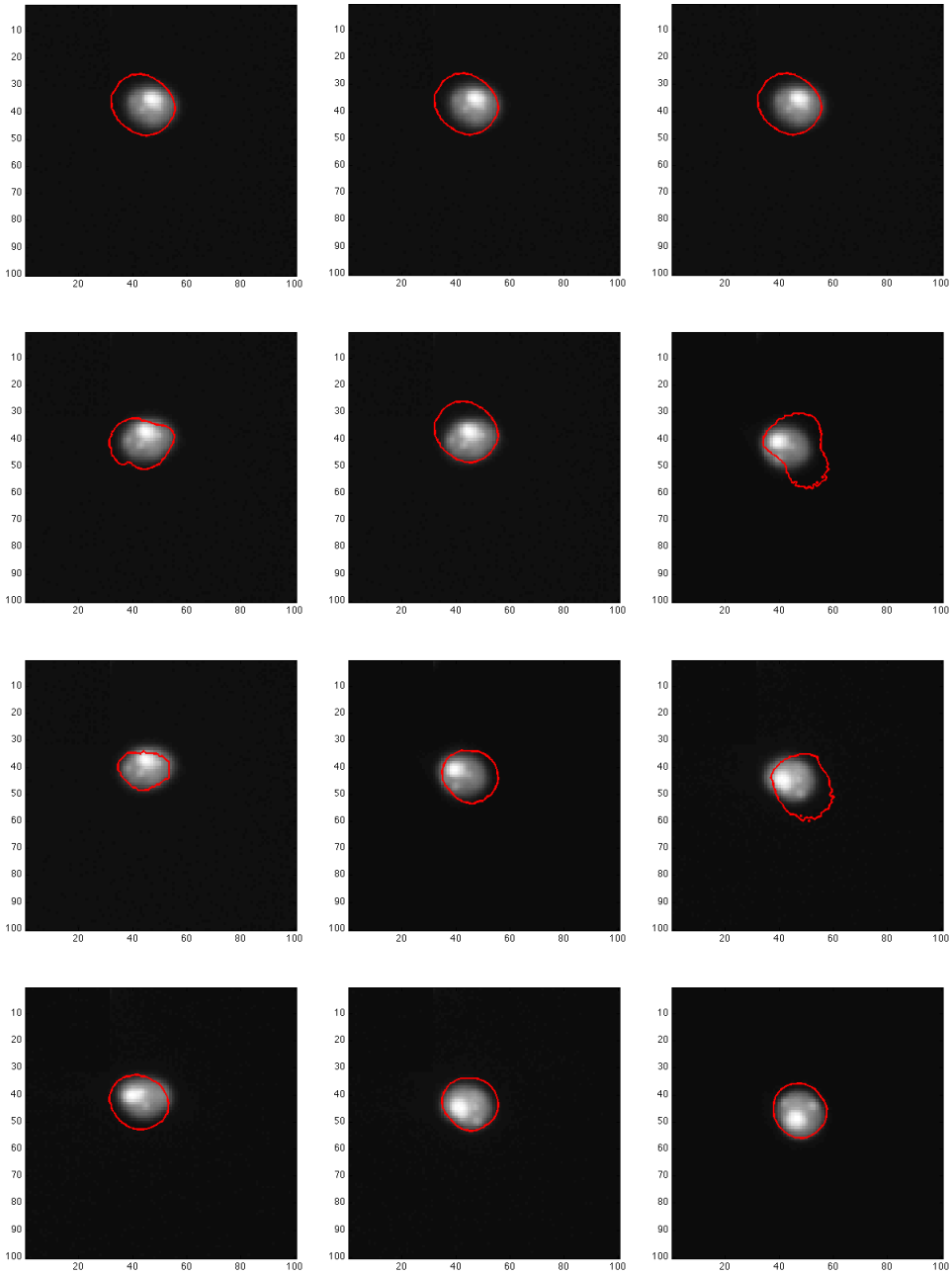

Figure 6. 3D-2D Segmentation results of image frames where a cell is removed from a gap of size (left) 6 frames, (middle) 11 frames, and (right) 16 frames.

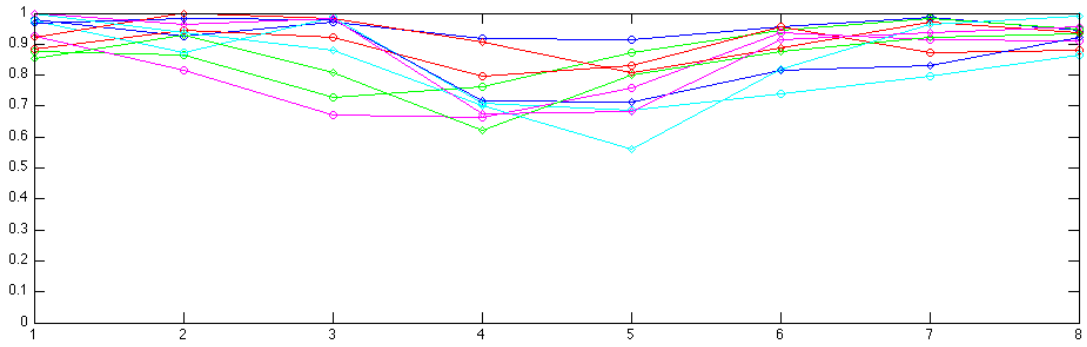

Figure 7. Accuracy of 3D-2D segmentation for 10 testing cases, each with a gap of 8 frames.

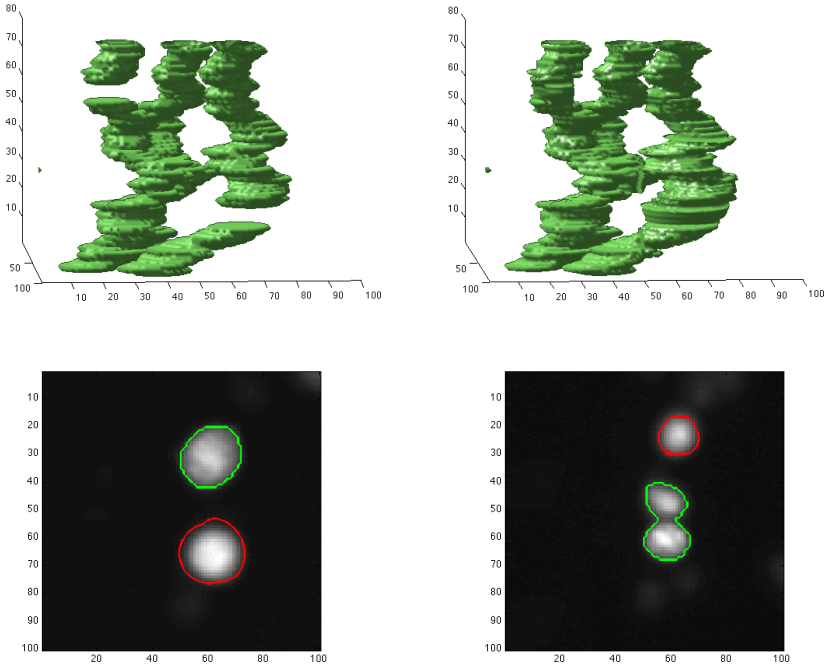

Figure 8. Segmentation of multiple cells with 2 gaps of height 7. The green contours are for visible cells and red contours for cells in the gaps.

[3] Zimmer, C., Labruyere, E., Meas-Yedid, V., Guillen, N., and Olivo-Marin, J., "Segmentation and tracking of migrating cells in videomicroscopy with parametric active contours: A tool for cell-based drug testing," *IEEE Transactions on Medical Imaging* **21**, 1212–1221 (2002).

[4] Zhang, B., Zimmer, C., and Olivo-Marin, J., "Tracking fluorescent cells with coupled geometric active contours," in [*Proceedings of IEEE International Symposium on Biomedical Imaging*], 476–479 (2004).

[5] Li, K., Miller, E. D., Weiss, L. E., Campbell, P. G., and Kanade, T., "Online tracking of migrating and proliferating cells imaged with phase-contrast microscopy," in [*Proceedings of the 2006 Conference on Computer Vision and Pattern Recognition Workshop (CVPRW '06)*], 65–72, IEEE Computer Society (June 2006).

[6] Ambriz-Colin, F., Torres-Cisneros, M., and Avina-Cervantes, J. G., "Detection of biological cells in phase-contrast microscopy images," in [*Proceedings of the Fifth Mexican International Conference on Artificial Intelligence (MICAI '06)*], 68–77, IEEE Computer Society (November 2006).

[7] Kenong, W., Gauthier, D., and Levine, M., "Live cell image segmentation," *IEEE Transactions on Biomedical Engineering* **42**, 1–12 (1995).

[8] Chan, T. F. and Vese, L. A., "Active contours without edges," *IEEE Transactions on Image Processing* **10**, 266–277 (2001).

[9] Osher, S. and Sethian, J. A., "Fronts propagating with curvature-dependent speed: Algorithms based on Hamilton-Jacobi formulation," *J. Comput. Phys.* **79**, 12–49 (1988).